Insertion Devices

1. Summary of Insertion Devices Operating at SPring-8

At present, fifteen insertion devices (IDs) have been installed and operated successfully. Eleven of these IDs are in-vacuum type, which is the most important feature of the ID program at SPring-8. Table 1 lists the performances of all of the IDs. The spectra obtained from those IDs are shown in Fig. 1.

1.1 Standard In-vacuum X-ray Undulators

Most of the X-ray applications populate the photon energy region from 8 keV to 16 keV. To meet this requirement, we have constructed 9 in-vacuum undulators having the same design. Therefore, they are called standard in-vacuum X-ray undulators. The undulator magnet array is composed of NdFeB permanent magnets with a period length of 32 mm, 140 periods and the maximum field of 0.85 tesla at the minimum gap of 8 mm. To obtain compatibility with UHV, the permanent magnets having high coercivity are coated with TiN. With a beam energy of 8 GeV, the fundamental of the radiation can cover the energy range from 5 keV to 18 keV, and higher harmonics, up to the 5th, can cover the range up to 80 keV. Figure 2 shows one of the standard in-vacuum X-ray undulators installed in the straight section of SPring-8.

1.2 In-vacuum Undulator for Industrial Application

To extend the available photon energy down to 4 keV, the undulator was designed to have a period length of 40 mm, which is somewhat longer than that of the standard type.

1.3 In-vacuum X-ray Hybrid Undulator

To obtain high photon energy with the fundamental, we constructed a special in-vacuum hybrid undulator composed of NdFeB magnets and permendur poles. The period length is as short as 24 mm so that the fundamental may cover the energy range up to 25 keV. The maximum field can be obtained as 1.1 tesla at a gap of 5 mm.

1.4 In-vacuum Tandem Vertical Undulator

The in-vacuum tandem vertical undulator is composed of two identical units for producing vertically polarized X-rays having different photon energies on the same axis. The periodic length is 3.7 cm and the number of periods per unit is 37. The attached beamline for structural biology is designed to make the best use of vertical polarization. Figure 3 shows the in-vacuum tandem vertical undulator installed in the storage ring.

1.5 Soft X-ray Figure-8 Undulator

The magnet structure of the figure-8 undulator is shown schematically in Fig. 4. The undulator is composed of six magnet arrays. The outer four magnet arrays generate horizontal field and the central two arrays generate vertical field. The period length of the horizontal field is twice as long as that of the vertical, so the electron trajectory projected in the transverse plane looks like a figure of 8. Therefore, this device is called a figure-8 undulator. As a result, the central power density is very low, which minimizes damage of the soft X-ray optical components.

1.6 In-vacuum Figure-8 Undulator

Originally, the figure-8 undulator design was developed to obtain a special radiation having a low central power density like that of a helical undulator; this is the most important characteristic of the figure-8 design. However, this type has another important characteristic: both horizontal and vertical polarizations are available. The integer/half odd-integer harmonics are polarized horizontally / vertically. The attached beamline is designed to utilize this unique characteristic. Figure 5 shows the magnet unit coated with TiN.

Table 1. Insertion devices in operation

	λu mm	N	G_{min} mm	B_{max} T	K_{max}	Pol.	n=1 keV	n=3 keV	n=5 keV	Beamline
Standard In-Vac X-ray U	32	140	8	0.84	2.5	hor.	4.8-18.5	14.5-51	24-80	BL09, 10, 11, 29, 39, 41, 44, 47
In-Vac U (Industrial Appl.)	40	112	15	0.59	2.2	hor.	4.4-14.5	13.3-40	22-60	BL16
In-Vac Hybrid U	24	187	5	1.1	2.6	hor.	6.6-25	20-70	34-100	BL46
In-Vac Tandem Vertical U	37	2×37	8	0.5	1.7	ver.	6.6-16	20-40	33-70	BL45
In-Vac Figure-8 U	26 52	172 86	5	1.05 0.34	2.6 1.7	hor. ver.	4.1-20			BL24
SX Figure-8 U	100 200	44 22	30	0.74 0.23	6.9 4.3	hor. ver.	0.17-5.8			BL27
SX Helical U	120	2×12	30	0.41	4.6	cir.	0.22-5			BL25
SX Helical U	120	16				cir.	0.3-5			BL23
Elliptical Wiggler	120	37	20	1.17 0.11	13.1 1.24	cir.				BL08

1.7 Soft X-ray Helical Undulator

The device is composed of two helical undulators having an opposite helicity. This configuration makes it possible to switch the helicity of circular polarization by using five kicker magnets. The target of the switching speed is 10 Hz. At present, we are trying various materials for pole pieces. The best material is thought to be laminated permalloy, which has a very low coercivity.

1.8 Elliptical Wiggler

As shown in Fig. 6, the principle is almost the same as that of the helical undulator except for the phasing system. The phase can be changed by translating the outer magnet arrays. This translating system operates efficiently because each array can be sifted independently. Therefore, we can adjust the net magnetic force on the central array to be always zero. Therefore, operation of the gap or phase is made by SR users.

2. Operational Experience with the IDs

2.1 Effects on the Closed Orbit

To realize independent tuning or user operation of the undulator, the closed orbit distortion derived from the undulator operation should be corrected. This correction is made by using steering magnets located at both ends of the undulator. To evaluate the effect of undulator operation, Fourier transformation is applied to the COD data, and the real and imaginary components for various gap values are obtained. The purpose is to minimize the variation of the Fourier components during the gap operation. However, it should be noted that these Fourier components include the natural drift of the stored beam due to the accelerator itself. Therefore, the quality of the correction depends on the accelerator performance with respect to the stability of the closed orbit. The lower part of Fig. 7 shows the variation in the imaginary part when the gap is closed from 50 mm to 8 mm and opened again to 50 mm. The dotted curve denotes the variation before correction and the solid curve after correction. The variation is greatly minimized by the correction. The upper part shows the variation in the real part, which is also minimized by the correction. However, drift due to the accelerator itself was also found. Figure 8 shows the COD caused by the undulator operation before or after correction by steering magnets. As shown in Fig. 8, the distortion is greatly reduced; the positional drift of the beam during gap operation from 8 mm to 50 mm was reduced down to less than 6 μm horizontally and 3 μm vertically. The directional drift was also reduced to less than 2 μrad horizontally and 0.3 μrad vertically.

2.2 Vacuum Behavior

Figure 9 shows the vacuum behaviors in the in-vacuum undulator of the standard type as well as the temperature of the components inside the vacuum. The abscissa represents elapsed time. The ordinate represents beam current, magnetic gap, vacuum pressure, RF-finger temperature, and magnet temperature. The beam injection is made once a day. The initial current was 70 mA, which after one day decreased down 35 mA. The operating gap ranged from 8 mm to 20 mm. The maximum pressure was 3×10^{-8} Pa. As the Figure shows, the pressure increased slightly when the gap was closed to a shorter value. The RF-finger temperature also closely corresponds to the beam current. The maximum temperature is 37 ˚C. The variation in the magnet temperature shows a small dependence on the beam current. Therefore, the vacuum system for the in-vacuum undulator seems to operate effectively.

2.3 Effects on the Beam Lifetime

In the ordinary case, the beam lifetime is expected to become shorter when the magnet gap of an in-vacuum undulator is closed, which originates from the beam loss due to the coulomb scattering of stored electrons by residual gases. However, it should be noted that the gap operation may change such beam parameters as the betatron tune, intensity of the skew fields, non-linear fields and resistive wall impedance. As a result, the volume of the bunch may be made larger, which makes Touschek lifetime longer. At SPring-8, we have sometimes found that the lifetime becomes longer when the gap is closed. Figure 10 shows the variation in the beam lifetime during gap operation of a standard in-vacuum undulator. The gap was closed from the maximum of 50 mm to the minimum of 8 mm and opened again to the maximum. As shown in Fig. 10, the lifetime is not a simple function of the gap value. Figure 11 shows another example, the case of vertical undulators producing vertically polarized radiation. The beam lifetime was made somewhat longer when the gap was closed from the maximum to 15 mm. The emittance coupling of the storage ring is estimated to be very low at 0.1 %. Therefore, we speculate that the emittance coupling could be easily increased when the gap is closed. As a result, Touschek lifetime can apparently be lengthened.

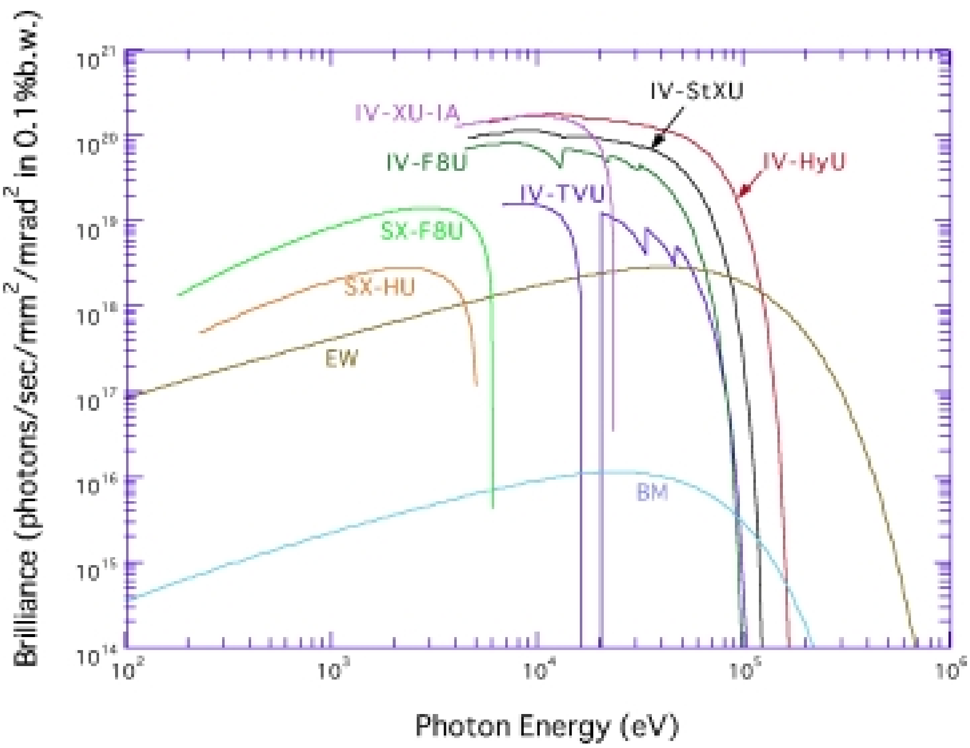

Fig. 1. Spectral brilliances obtained from insertion devices at SPring-8. Beam parameters: beam energy: 8 GeV, beam current: 100 mA, emittance: 7 nm•rad, emittance coupling: 0.1 %. Spectra from standard in-vacuum X-ray undulator is denoted by IV-StXU, in-vacuum hybrid undulator by IV-HyU, in-vacuum undulator for industrial applications by IV-XU-IA, in-vacuum tandem vertical undulator by IV-TVU, in-vacuum figure-8 undulator by IV-F8U, soft X-ray figure-8 undulator by SX-f8U, soft X-ray helical undulator by SX-HU, elliptic wiggler by EW, and bending magnet by BM.

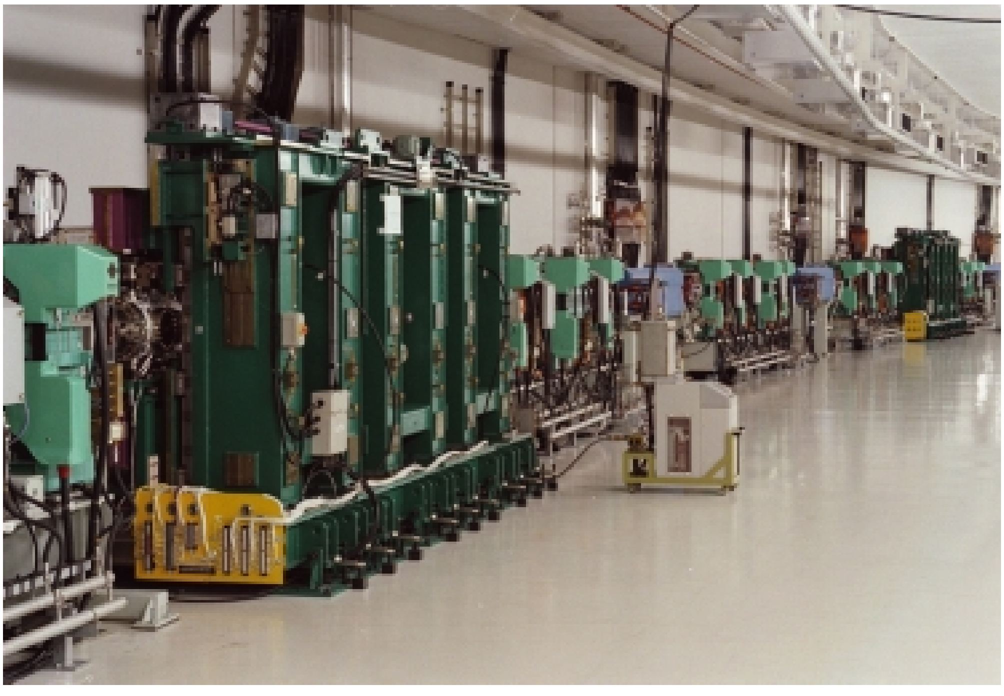

Fig. 2. One of the standard in-vacuum undulators installed in the straight section of the SPring-8 ring.

Fig. 3. In-vacuum tandem vertical undulator.

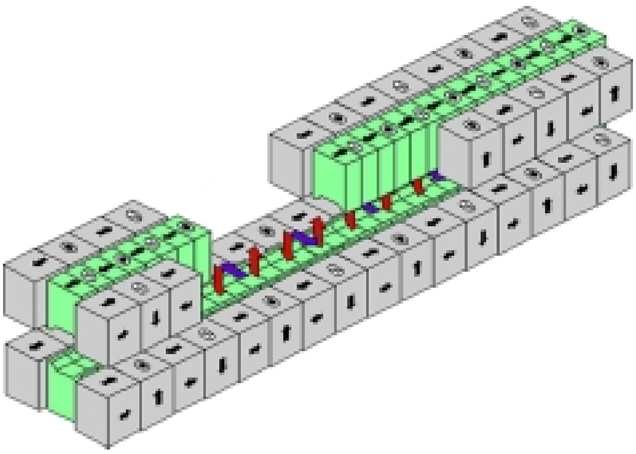

Fig. 4. Principle of figure-8 undulator design.

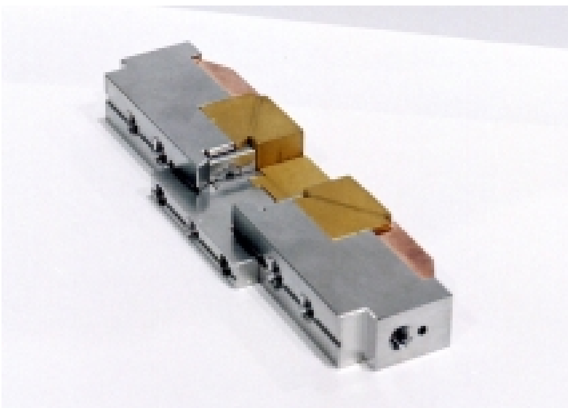

Fig. 5. Magnet unit for in-vacuum figure-8 undulator.

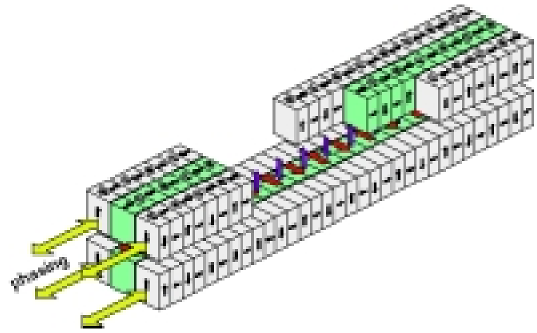

Fig. 6. Principle of elliptic wiggler design.

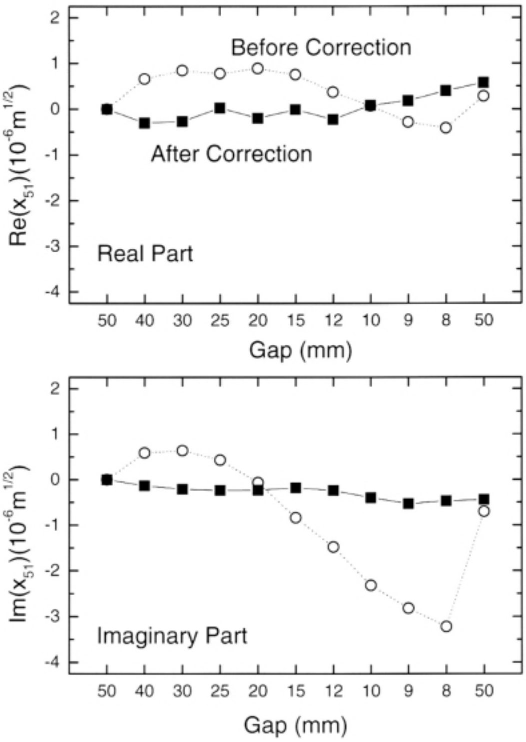

Fig. 7. Fourier components obtained from COD data before and after correction.

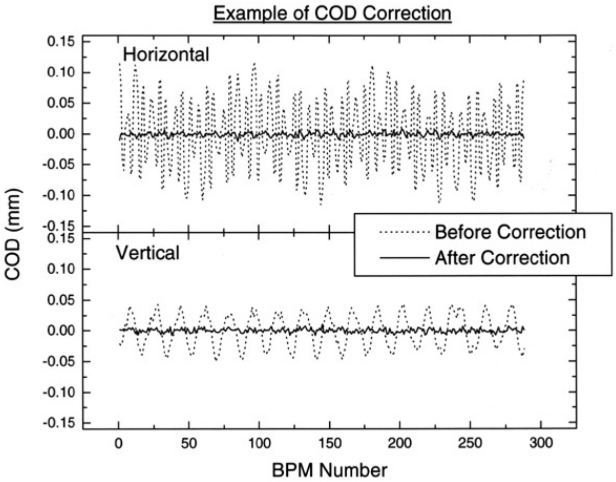

Fig. 8. COD data around the ring before and after correction.

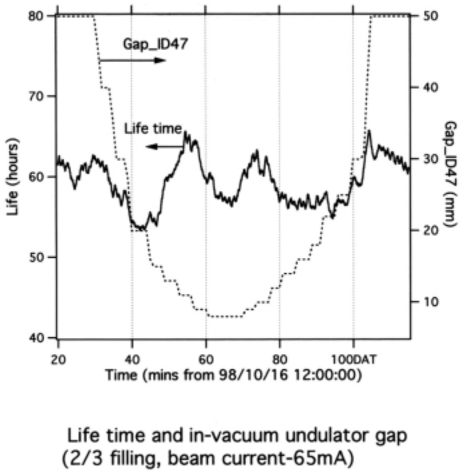

Fig. 10. Behavior of beam lifetime during gap operation of standard in-vacuum X-ray undulator.

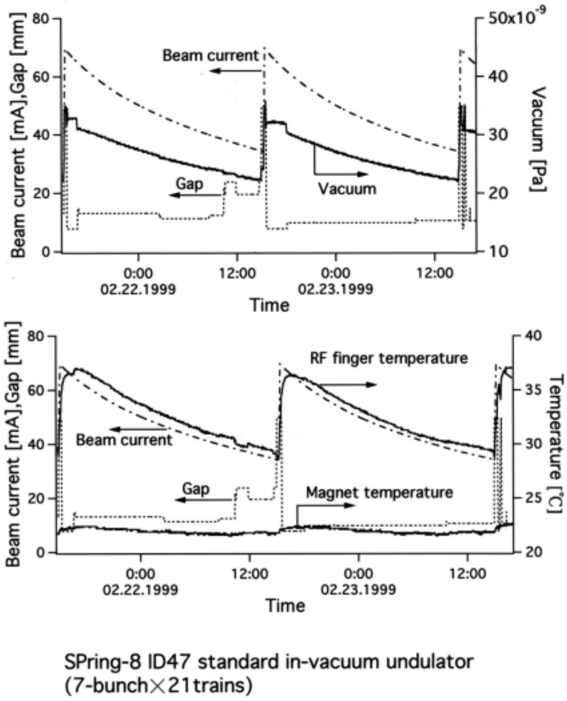

Fig. 9. Vacuum and temperature behaviors for the standard in-vauum undulator.

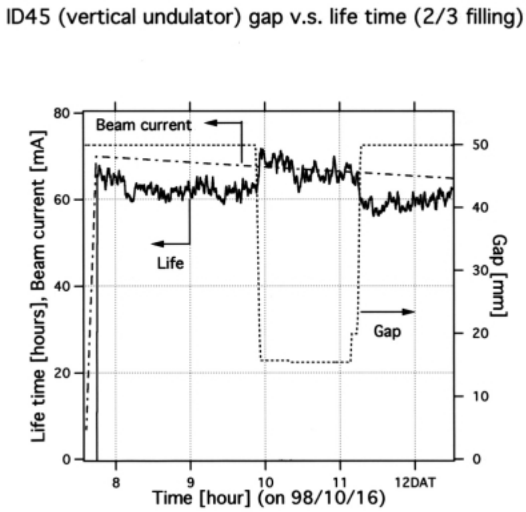

Fig. 11. Behavior of beam lifetime during gap operation of in-vacuum tandem vertical undulator.